National Park Service
U.S. Department of the Interior

Yosemite Valley, El Capitan (left), and Half Dome (center), Yosemite National Park (photo P. Gonzalez)

Climate Change Trends, Vulnerabilities, and Carbon in Yosemite National Park, California, USA

Patrick Gonzalez, Ph.D.

Natural Resource Stewardship and Science
U.S. National Park Service
130 Mulford Hall
University of California, Berkeley
Berkeley, CA 94720-3114 USA

February 9, 2016

Abstract

Greenhouse gas emissions from human activities have caused global climate change and widespread impacts on physical and ecological systems. To assist in the integration of climate change science into resource management in Yosemite National Park (N.P.), this report presents: (1) results of original spatial analyses of historical and projected climate change trends at 800 m spatial resolution, (2) results of a systematic scientific literature review of historical impacts, future vulnerabilities, and ecosystem carbon, focusing on research conducted in the park, and (3) results of original spatial analyses of ecosystem carbon at 30 m spatial resolution. For the area within park boundaries, average annual temperature from 1950 to 2010 increased at a statistically significant rate of 1.9 ± 0.7ºC (3.4 ± 1.3ºF.) per century (mean ± standard error), with the greatest increase in spring. Total annual precipitation from 1950 to 2010 showed no statistically significant change. Measurements from 1911 to 2015 at the weather station at Hetch Hetchy showed similar trends. Published analyses of field research that includes data from Yosemite N.P. detected changes that have been attributed to human climate change. These impacts include snowpack reductions, advance of spring warrmth, tree dieback, wildfire changes, and upslope shifts of vegetation biomes and small mammal ranges. If the world does not reduce greenhouse gas emissions, projections under the four emissions scenarios of the Intergovernmental Panel on Climate Change (IPCC) indicate annual average temperature increases of up to 4.7 ± 1.0ºC (8.5 ± 1.8º F.) (mean ± standard deviation) from 2000 to 2100 for the park as a whole. Climate models project increases of total annual precipitation of 3% to 6% on average, but many individual models project decreases. Published analyses for the area including the national park identify numerous vulnerabilities to future climate change, including more upslope biome shifts, increases in wildfire, changes in stream flow, persistence of invasive yellow starthistle (*Centaurea solstitialis*), and reduction of the ranges of pika (*Ochotona princeps*) and other wildlife. National park ecosystems can help to naturally reduce climate change by storing carbon. Aboveground vegetation in the park stores an amount of carbon equivalent to the annual emissions of 2.6 ± 1.4 million Americans (mean ± 95% confidence interval). From 2001 to 2010, total aboveground carbon in the park fell 8 ± 4%, with most of the carbon loss from areas that burned in wildfire, where a century of fire suppression has caused a buildup of fuels.

Introduction

Greenhouse gas emissions from power plants, motor vehicles, deforestation, and other human activities have increased temperatures around the world and caused other changes in climate in the 20th and early 21st centuries (IPCC 2013). Field measurements show that climate change is fundamentally altering ecosystems by shifting biomes, contributing to species extinctions, and causing numerous other changes (IPCC 2014). To assist Yosemite N.P. in the integration of climate change science into resource management, this report presents results of original spatial analyses of historical and projected climate change and ecosystem carbon and a summary of published scientific findings on climate change impacts and vulnerabilities and ecosystem carbon.

The historical analyses (Wang et al., in preparation) use previously published spatial climate data layers at 800 m spatial resolution, derived from point weather station measurements using the Parameter-elevation Relationships on Independent Slopes Model (PRISM; Daly et al. 2008). This data set uses weather station measurements and interpolates between weather stations based on elevation and topography. The spatial analysis area is the area within park boundaries. Linear regression of temperature and precipitation time series gives the historical climate trends, with the statistical probability of significance corrected for temporal autocorrelation.

The spatial analyses of future projections (Wang et al., in preparation) use output of all available general circulation models (GCMs) of the atmosphere in the Coupled Model Intercomparison Project Phase 5 (CMIP5) data set established for the most recent IPCC report (IPCC 2013). The coarse GCM output, often at spatial resolutions of up to 200 km, has been downscaled to 800 m spatial resolution using bias correction and spatial disaggregation (BCSD; Wood et al. 2004).

The information on climate change impacts and vulnerability comes from a search of the Thomson Reuters Web of Science scientific literature database for published research that used field data from Yosemite N.P. or spatial analyses of the region that includes the park.

Historical Climate Changes

For Yosemite N.P. as a whole, mean annual temperature showed statistically significant increases in the periods 1895-2010, 1950-2010, and 1950-2013 (Figure 1, Table 1). The periods starting in 1950 give more robust time series than the period starting in 1895 because the United States (U.S.) Government established a substantial number of weather stations in the late 1940s and the weather station network has been relatively stable since then. Spatial data from the longer period relies on fewer weather stations and a network that enlarged irregularly before the 1940s. The 1950-2010 trends show statistically significant warming in spring and summer with the greatest rate of warming in spring (Table 1). The highest rates of warming have occurred in upper elevations north of the Tuolumne River and around Tuolumne Peak (Figure 2).

The park hosts three currently operating National Weather Service Cooperative Observer Program weather stations (Davey et al. 2007). The weather station at Hetch Hetchy shows statistically significant warming of 1.1 ± 0.3ºC per century for the period 1911-2015 (Figure 1). Due to data gaps, the Park Headquarters and South Entrance weather stations provide data that is less reliable for long-term trend analysis. A previous NPS report (Edwards and Redmond 2011) identified how this problem is particularly negative for the Yosemite N.P. Headquarters weather station since it was established in 1905, earlier than many weather stations around the world.

The Hetch Hetchy weather station and other stations across the western U.S. have provided data for the detection of global climate change in the last half of the 20th century and the attribution to emissions from human activities. Changes in climate in the western U.S. include increases in winter minimum temperatures at rates of 2.8 to 4.3ºC per century (Barnett et al. 2008, Bonfils et al. 2008) and decreased ratio of snow to rain at rates of -24 to -79% per century (Barnett et al. 2008, Pierce et al. 2008) from 1950 to 1999 and an advance of spring warmth of a week from 1950 to 2005 (Ault et al. 2011).

The Hetch Hetchy weather station is part of the Global Historical Climatology Network (Lawrimore et al. 2011) and has therefore contributed to the detection of increasing global average temperature, changes in global precipitation, and global increases in extreme temperature and precipitation events (IPCC 2013). In the U.S., the number of warm nights per year (minimum daily temperature >90th percentile) increased by up to 20 days from 1951 to 2010 (IPCC 2013).

For Yosemite N.P. as a whole, total annual precipitation for the periods 1950-2010 and 1950-

2013 showed no statistically significant trends, with the precipitation slightly increasing in the shorter time series and slightly decreasing in the longer time period (Figure 3, Table 2). For the period 1950-2010, precipitation increased on 71% of park surface area and decreased on 22% (Figure 4). Precipitation at the Hetch Hetchy weather station from 1911 to 2015 did not show a statistically significant trend.

National Oceanic and Atmospheric Administration (NOAA) analyses of weather station data show an increase in the southwestern U.S. of heavy storms, with the decade 1991-2000 experiencing an increase of 25% in five-year storms (a storm with more precipitation than any other storm in five years), compared to the 1901-1960 average (Walsh et al. 2014). NOAA analyses show a 5% increase in the amount of precipitation falling in the heaviest 1% of all daily storm events from 1958 to 2012 in the southwestern U.S. (Walsh et al. 2014).

Historical Impacts

Changes detected in Yosemite N.P. and attributed to human climate change Published research using field data from Yosemite N.P. has detected ecological changes statistically significantly different from historic variation and attributed the cause of those changes to human climate change and not other factors.

Tree dieback Tracking of trees in permanent old-growth conifer forest plots across the western U.S., including plots in Yosemite N.P., found a statistically significant doubling of tree mortality between 1955 and 2007 (van Mantgem et al. 2009). Analyses of fire, mortality of small trees, forest fragmentation, air pollution, and climate attributed the mortality to warming due to climate change.

Wildfire Multivariate analysis of wildfire across the western U.S. from 1916 to 2003, using data from Yosemite N.P. and other areas, indicates that climate was the dominant factor controlling the extent of burned area, even during periods of active fire suppression (Littell et al. 2009). Reconstruction of fires of the past 400 to 3000 years in the western U.S. (Marlon et al. 2012, Trouet et al. 2010) and in Sequoia and Yosemite National Parks (Swetnam 1993, Swetnam et al. 2009, Taylor and Scholl 2012) confirm that temperature and drought are the dominant factors explaining fire occurrence.

Biome shift Field surveys in Tuolumne Meadows, Mammoth Peak, and other sites in Yosemite N.P. and adjacent national forests found that subalpine forest shifted upslope into subalpine meadows between 1880 and 2002, attributable to climate change and not the Pacific Decadal Oscillation (Millar et al. 2004).

Wildlife range shifts Small mammal resurveys from 2003 to 2006 of the Grinnell surveys from 1914 to 1920 of a transect that crossed the center of Yosemite N.P. showed that the ranges of half of 28 small mammal species shifted upslope an average of ~500 m (Moritz et al. 2008). Because the national park had protected the survey transect, land use change or other factors were not major factors. Therefore, the authors attributed the shift to a 3°C increase in minimum temperature caused by climate change. Analyses of Audubon Christmas Bird Count data across the U.S., including a count circle in Yosemite N.P., detected a northward shift of winter ranges of a set of 254 bird species at an average rate of 0.5 ± 0.3 km per year from 1975 to 2004, attributable to human climate change (La Sorte and Thompson 2007).

Changes detected in the region and attributed to human climate change Measurements from National Weather Service stations and Natural Resources Conservation Service snow courses across the western U.S. detected decreased snowpack (Barnett et al. 2008, Pierce et al. 2008) and advances of spring stream flow of a week (Barnett et al. 2008) from 1950 to 1999.

Changes consistent with, but not formally attributed to human climate change Other research has examined observations consistent with, but not formally attributed to, human climate change. Some changes have only been observed and not detected (shown statistically significantly different than historical variability).

Higher-elevation tree increases Resampling in 2009 of Wieslander plots from 1920s and 1930s above 2300 m (7500 ft.) elevation in the Sierra Nevada, including plots in Yosemite N.P., found increases in subalpine tree densities (Dolanc et al. 2013). Analyses of whitebark pine (*Pinus albicaulis*) tree rings from cores taken around Mammoth Peak and other areas found an acceleration of growth after 1950 at rates greater than any time in the period 1000-1990 (Bunn et al. 2005).

Large tree decline Comparison of Wielslander plots from 1932 to 1936 with NPS plots from 1988 to 1992 in the park shows a decline in large trees (Lutz et al. 2009a), consistent with similar trends outside the park (McIntyre et al. 2015).

Wildfire increase From 1984 to 2005, tracking of fire ignitions and measurements of snowpack found substantial increases of lightning-ignited fires as snowpack decreased (Lutz et al. 2009b). Fire perimeters from the park and along the Sierra Nevada indicate a recent increase in the upper elevation of fires across the region (Schwartz et al. 2015).

Wildlife changes The resurvey of the Grinnell survey in Yosemite N.P. also recorded the pinyon mouse (*Peromyscus truei*) in the park for the first time, having expanded its range upslope from outside the park (Yang et al. 2011). Climate and vegetation explained the ranges of chipmunks (*Tamias spp.*), with climate dominant (Rubidge et al. 2011). Genetic diversity in the alpine chipmunk (*Tamias alpinus*) decreased as its lower elevation limit retracted (Rubidge et al. 2012). Half of the species in the resurvey in the park also showed shifts of associated vegetation types (Santos et al. 2015). Resurveys from 2003 to 2008 of the Grinnell surveys from the 1911 to 1929 in Lassen Volcanic N.P., Sequoia N.P., and Yosemite N.P. found elevation shifts of bird ranges ranges that tracked temperature and precipitation (Tingley et al. 2009, 2012). Other resurveys indicated that small mammal ranges shifted upslope or downslope for 25 of 34 species analyzed, depending on temperature (Rowe et al. 2015), Belding's ground squirrel (*Urocitellus beldingi*) was extirpated from 42% of sites as snow cover decreased (Morelli et al. 2012), and squirrel body size increased as food plant growing season lengthened (Eastman et al. 2012).

Future Climate Projections

IPCC has coordinated research groups to project possible future climates under four defined greenhouse gas emissions scenarios, called representative concentration pathways (RCPs; Moss et al. 2010). The four emissions scenarios are RCP2.6 (reduced emissions from increased energy efficiency and installation of renewable energy), RCP4.5 (low emissions), RCP6.0 (high emissions, somewhat lower than continued current practices), and RCP8.5 (highest emissions due to lack of emissions reductions).

If the world does not reduce emissions from power plants, cars, and deforestation by 40-70%, GCMs project substantial warming and slight increases in precipitation. The temperature and precipitation projections from 33 GCMs form a cloud of potential future climates (Figure 5). GCMs project potential increases in annual average temperature within park boundaries greater than historical 20th century warming by 2050 (Table 3) and up to double historical warming by 2100 (Table 4). Projected temperature increases do not show much spatial variation across the park (Figure 6). Models project the greatest temperature increases in the autumn (Tables 5, 6).

The average of the ensemble of GCMs projects increased precipitation under all emissions scenarios (Tables 5, 6). The average of the ensemble reflects the central tendency of the projections, but the uncertainty of any single model of future climate can be large. In the case of central California, the GCMs do not agree on precipitation projections, with over half projecting increases, but many projecting decreases (Figure 5). Projected precipitation increases tend to increase from wests to east, but do not show much spatial variation across the park (Figure 7).

Projections indicate potential changes in the frequency of extreme temperature and precipitation events. For central California, under the highest emissions scenario, models project up to 10 more days per year with a maximum temperature >35ºC (95ºF.) and an increase in 20-year storms (a storm with more precipitation than any other storm in 20 years) to once every 5-6 years (Walsh et al. 2014).

Future Vulnerabilities

If the world does not reduce emissions from power plants, cars, and deforestation, continued climate change could increase the vulnerability of physical and ecological resources (IPCC 2013). Published research in Yosemite N.P. or research that included the region of the park has identified numerous vulnerabilities.

Wildfire Under high emissions [IPCC (2000) emissions scenario A2], climate change could double or triple burned area in the region of the park between the periods 1961-1990 and 2071-2100 (Westerling et al. 2011). Under low emissions [IPCC (2000) emissions scenario B1], burned area could remain approximately the same or increase slightly. This demonstrates the positive impact of energy conservation, renewable energy, and other actions to reduce greenhouse gas emissions.

In the Sierra Nevada, because models diverge on whether precipitation may increase or decrease, two broad types of fire futures (Littell et al. 2009) under a high emissions scenario could be:

1. Dry-fire future – hotter and drier climate, increased fire frequency, fire limited by vegetation, potential biome change of forest to grassland after a fire due to low natural regeneration, high carbon emissions
2. Intense-fire future – hotter and wetter climate, more vegetation, increased fire frequency and intensity, fire limited by climate, higher carbon emissions.

These are two broad categories that each encompass a range of fire conditions. On the ground, gradients of temperature, precipitation, and climate water deficit (difference between precipitation and actual evapotranspiration) generate gradients of fire conditions.

Because climate change, vegetation, and ignitions vary across the landscape, potential fire frequency may show high spatial variability (Gonzalez et al. 2010b, Moritz et al. 2012, Westerling et al. 2011). Therefore, fire future types could appear in patches across the landscape, with different fire future types manifesting themselves in adjacent forest patches.

In the high-frequency, low-severity fire regimes of the Sierra Nevada, managed wildland fire and prescribed burning can reduce the potential for crown fires in both fire future types (Stephens et al. 2013). Due to a century of unnatural fire suppression, wildfires in California emitted more carbon from 2001 to 2010 than the forests absorbed through regrowth (Gonzalez et al. 2015). Although managed wildland fire and prescribed burning can release a pulse of carbon in the short-term, they can reduce net greenhouse gas emissions in the long-term because future carbon storage in trees, which can grow older and larger after wildland fire and prescribed burning, can outweigh the short-term emissions (Hurteau and North 2009b).

Vegetation Under low emissions, an increase in climate water deficit (a measure of aridity) may increase the vulnerability of western white pine (*Pinus monticola*) and mountain hemlock (*Tsuga mertensiana*) in the park to mortality (Lutz et al. 2010). Under all emissions scenarios, the west side of Yosemite N.P. is highly vulnerable to the combined effects of biome shifts due to climate change and habitat loss due to land cover change (Gonzalez et al. 2010b, Eigenbrod et al. 2015). Mock leopardbane (*Arnica dealbata*), a rare flowering plant, is vulnerable in the park to decreased snowpack and nitrogen deposition from air pollution (Hurteau and North 2009a).

Under high emissions, Yosemite will continue to be vulnerable to the invasive yellow starthistle (*Centaurea solstitialis*) (Bradley et al. 2009). Alpine fens (meadows fed by groundwater) in Sierra Nevada sites outside the park exhibit vulnerability to drying under increased temperatures (Drexler et al. 2013).

Streams Under high emissions, warmer winter temperatures could advance spring stream flow center of mass by one month in the Tuolumne River basin upstream of Tuolumne Meadows (Cristea et al. 2014). Decreased winter snowpack in the Merced River basin could substantially reduce summer stream flow (Godsey et al. 2014). An air temperature increase of 4ºC could substantially increase the time that stream temperatures in the park exceed 21ºC, a threshold for many cold water fish species, from almost no time, under current conditions, to up to 14 weeks (Null et al. 2013).

Wildlife Under high emissions, upslope and poleward shifting of cooler climates and biomes increases the vulnerability of the American pika (*Ochotona princeps*) to extirpation in Lassen Volcanic, Sequoia, and Yosemite National Parks (Stewart et al. 2015) and suitable habitat for Belding's ground squirrel (*Urocitellus beldingi*) could reduce substantially (Morelli et al. 2012). Projections of the ranges of 213 mammal species under high emissions indicate potential losses of six species from Yosemite N.P., including ringtail (*Bassaricus astutus*), and a potential influx of 25 species, half of them rodents (Burns et al. 2003). Of 164 bird species modeled throughout the Sierra Nevada, one species, the white-tailed Ptarmigan (*Lagopus leucura*), a species introduced into the park but uncommon, was ranked as extremely vulnerable under high emissions (Siegel et al. 2014).

Ecosystem Carbon

Growing vegetation naturally removes carbon from the atmosphere, reducing the magnitude of climate change. Conversely, deforestation, wildfire, and other agents of tree mortality emit carbon to the atmosphere, exacerbating climate change. Determining the balance between ecosystem carbon emissions to the atmosphere and removals from the atmosphere is essential for tracking the role of ecosystems in climate change (IPCC 2013). Analyses of Landsat remote sensing and field measurements of biomass across the state of California have produced estimates of the carbon in aboveground vegetation for the grasslands, woodlands, forests, and other non-agricultural and non-urban areas of the state at 30 m spatial resolution (Gonzalez et al. 2015). Monte Carlo analyses of error in tree measurements, remote sensing, and the carbon fraction of biomass quantified the uncertainty of carbon stock change estimates. Validation of the carbon stock estimates by independent measurement-derived stocks at field sites and matching of forest carbon stock estimates with other remote sensing-derived stocks indicated the skill of the carbon estimation methods.

In 2010, aboveground live vegetation in Yosemite N.P. contained 14.8 ± 7.9 million tons of carbon (Table 7) (Gonzalez et al. 2015). This stock is equivalent to the greenhouse gases emitted in one year by 2.6 ± 1.4 million Americans. The highest carbon densities Yosemite N.P. occur in the Mariposa Grove of giant sequoias (*Sequoiadendron giganteum*), in red fir (*Abies magnifica*) forests, and in the other conifer forests of the west slope of the Sierra Nevada (Figure 8). Giant sequoia forest can attain aboveground live carbon densities up to 2200 tons per hectare (Blackard et al. 2008) while Sierra Nevada red fir can attain 360 ± 80 tons per hectare (Gonzalez et al. 2010a).

Using field measurements in Yosemite N.P. and different methods, Matchett et al. (2015) estimated a higher aboveground tree carbon stock for Yosemite N.P. of 25 ± 2 million tons. The stocks showed similar spatial patterns across the park, but the Matchett et al. (2015) estimates were consistently higher. They found carbon densities of 500 ± 150 tons per hectare in Giant sequoia trees and 300 ± 70 tons per hectare in red fir trees.

Based on measurements in the parks at Dana Meadows, subalpine meadows contain carbon in aboveground vegetation at 0.5 to 4.5 tons per hectare (Arnold et al. 2014). Based on soil cores at three montane fens (meadows fed by groundwater) in the park, soil organic carbon densities ranged from 54 to 100 tons per hectare (Drexler et al. 2015). So, most of the carbon in those types of meadows are below ground. Monitoring of snowpack and meadow carbon dioxide fluxes for three years, Arnold et al. (2014) found that soil carbon losses doubled when snowpack declined by more than half and higher temperatures increased the growing season by two months.

From 2001 to 2010, aboveground vegetation carbon increased on 8% of the land area of Yosemite N.P. and decreased on 15% (Figure 8; Gonzalez et al. 2015). The carbon increases result from increased vegetation cover and tree height. The carbon decreases occurred mainly in areas burned by wildfire and, to a lesser extent, by prescribed burns. Across the western U.S., a century of fire suppression has depressed fire frequencies below natural levels and caused substantial increases in the densities of small-diameter trees and accumulations of dead matter that serve as fuel (Stephens et al. 2007, Marlon et al. 2012). A short-term emissions increase may be difficult to avoid because NPS and other agencies use wildland fire and prescribed burning to restore ecologically appropriate fire regimes to the land. Moreover, if the world does not reduce greenhouse gas emissions from cars, power plants, and other fossil fuel-burning human activities, projections indicate that climate change may double or triple burned area in the region of the park by 2085 under a high emissions scenario (Westerling et al. 2011). Although some fire management practices may release greenhouse gases in the short term, they can augment carbon storage in the long term by changing forests with many stands of small trees to one dominated by fewer large, old trees (Hurteau and Brooks 2011, Earles et al. 2014, Hurteau et al. 2014).

Yosemite N.P. has conducted an inventory of greenhouse gas emissions from fossil fuel use in buildings and vehicles (Villalba et al. 2013) as part of the NPS Climate Friendly Parks program to reduce park fossil fuel emissions. The carbon equivalent of emissions from buildings and vehicles in the park, electricity imported from outside the park, and commuting of employees and waste management increased from 34 000 to 35 000 tons from 2008 to 2011, but the emissions per visitor fell from 10 to 9 tons per visitor from 2008 to 2011 (Villalba et al. 2013).

Figure 1.

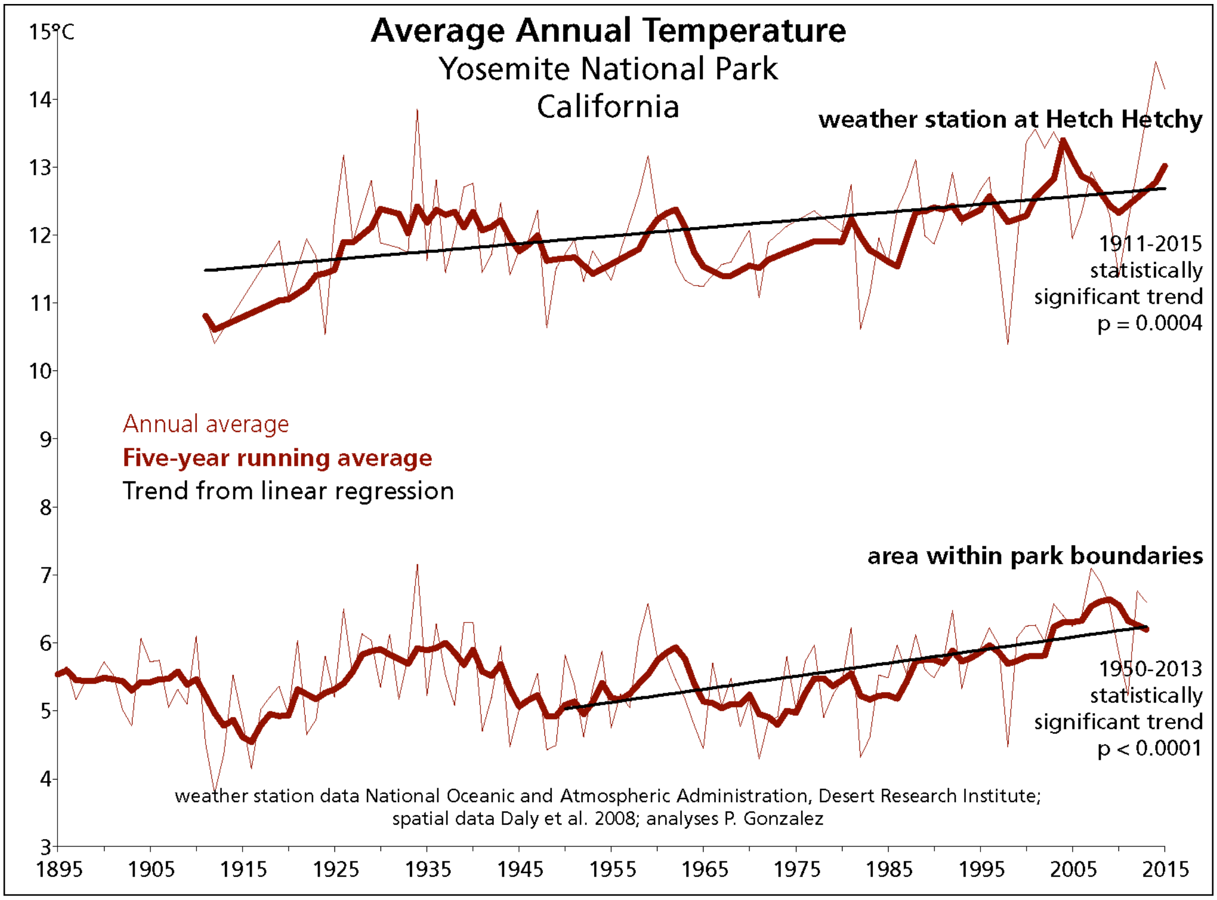

Note that, for the spatial data (bottom graph of the area within park boundaries), the period 1950-2013 gives a more robust time series than the period 1895-2013. The U.S. Government established a substantial number of weather stations in the late 1940s and the weather station network has been relatively stable since then. Spatial data from the longer period relies on fewer weather stations and a network that enlarged irregularly before the 1940s.

Figure 2.

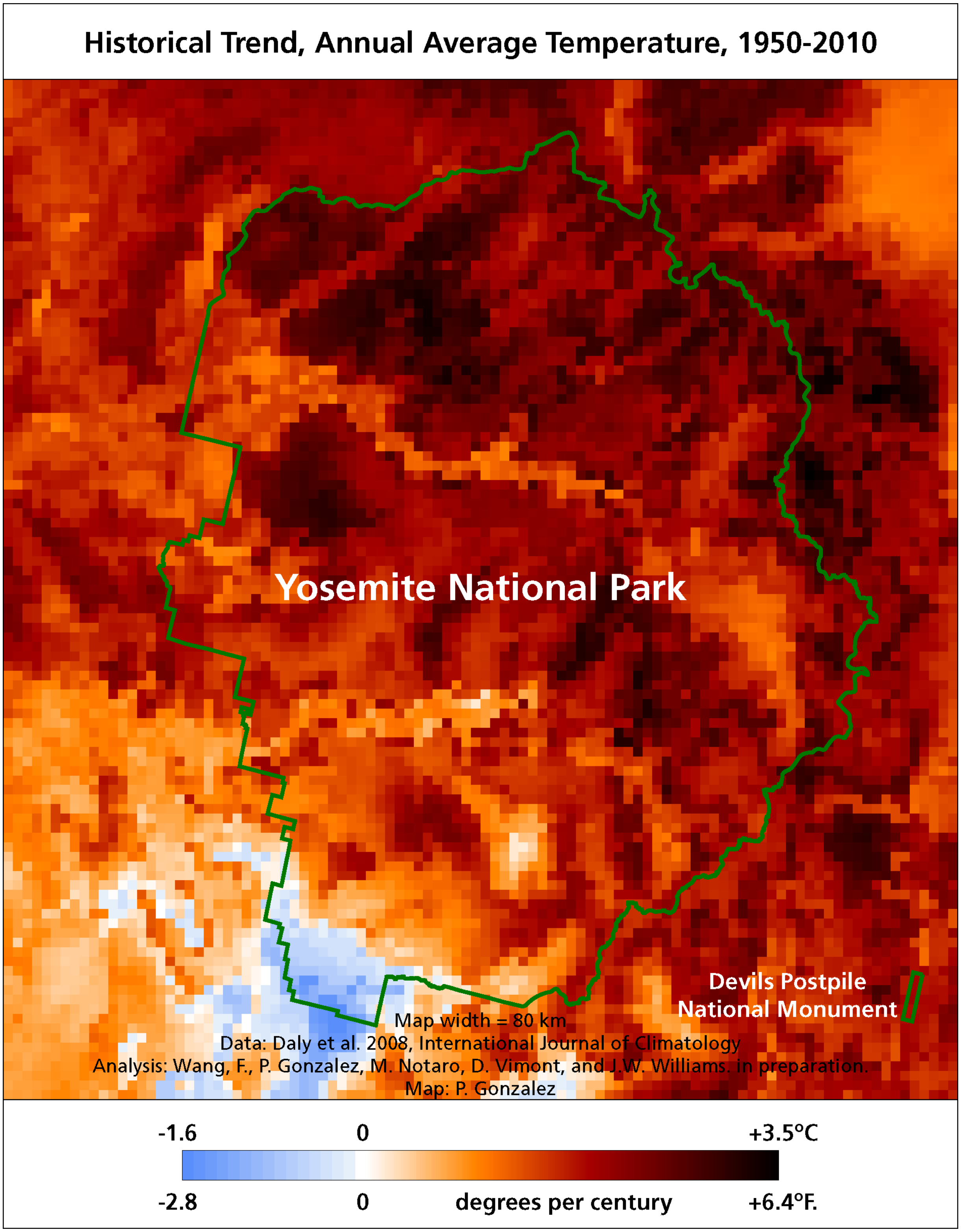

Minimum -1.6°C, Maximum 3.5°C per century

Figure 3.

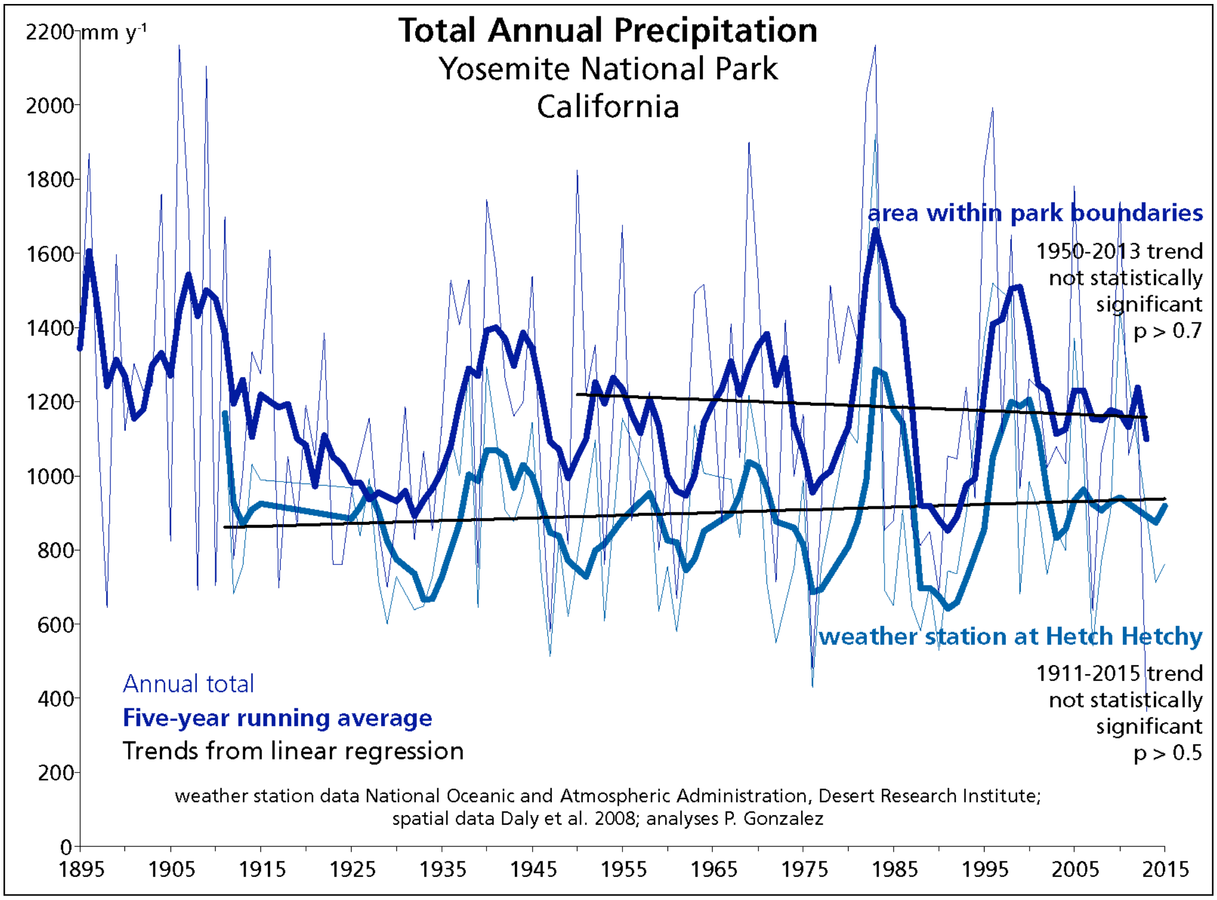

Note that, for the spatial data (top graph of the area within park boundaries), the period 1950-2013 gives a more robust time series than the period 1895-2013. The U.S. Government established a substantial number of weather stations in the late 1940s and the weather station network has been relatively stable since then. Spatial data from the longer period relies on fewer weather stations and a network that enlarged irregularly before the 1940s.

Figure 4.

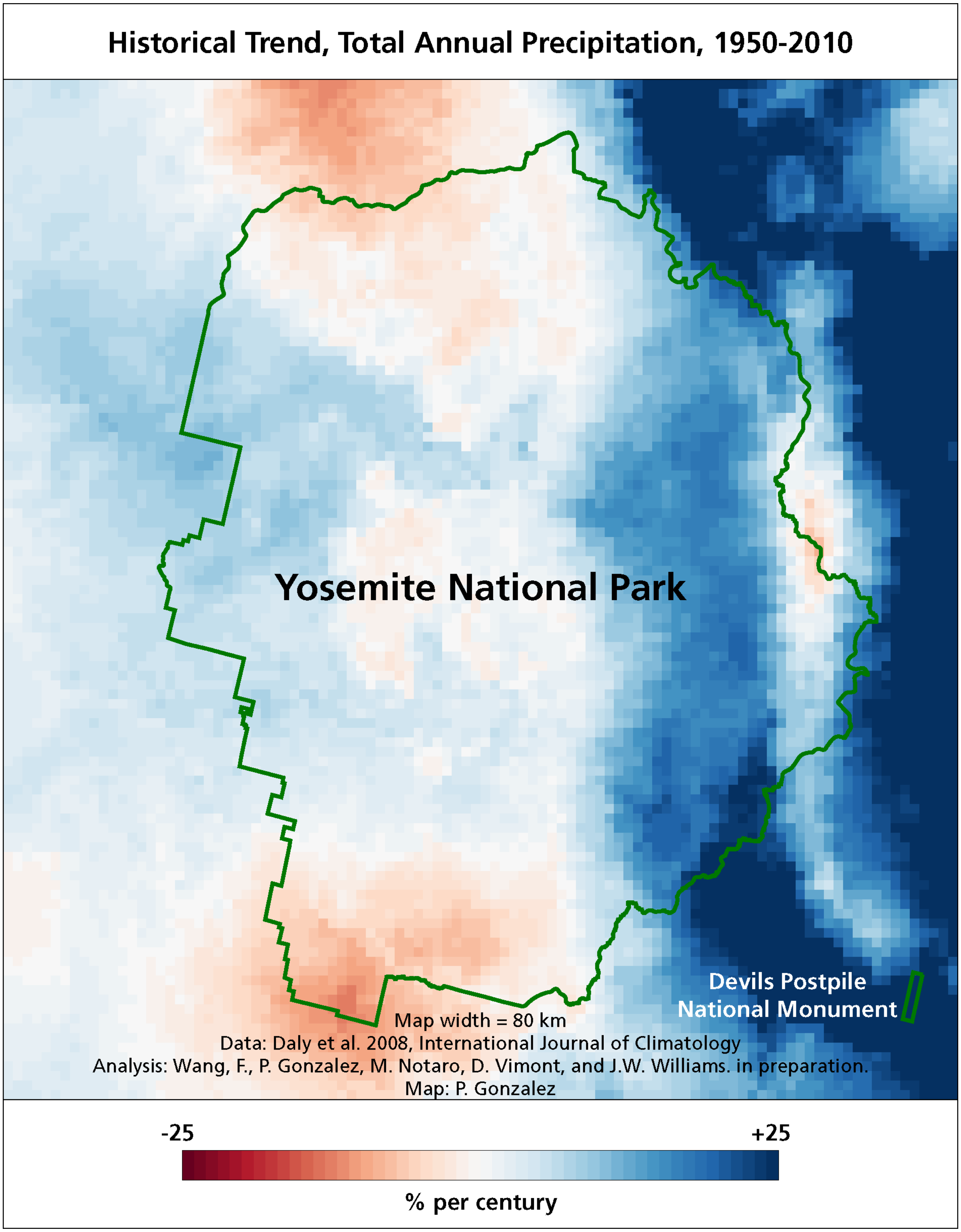

Minimum -13%, Maximum +52% per century

Figure 5.

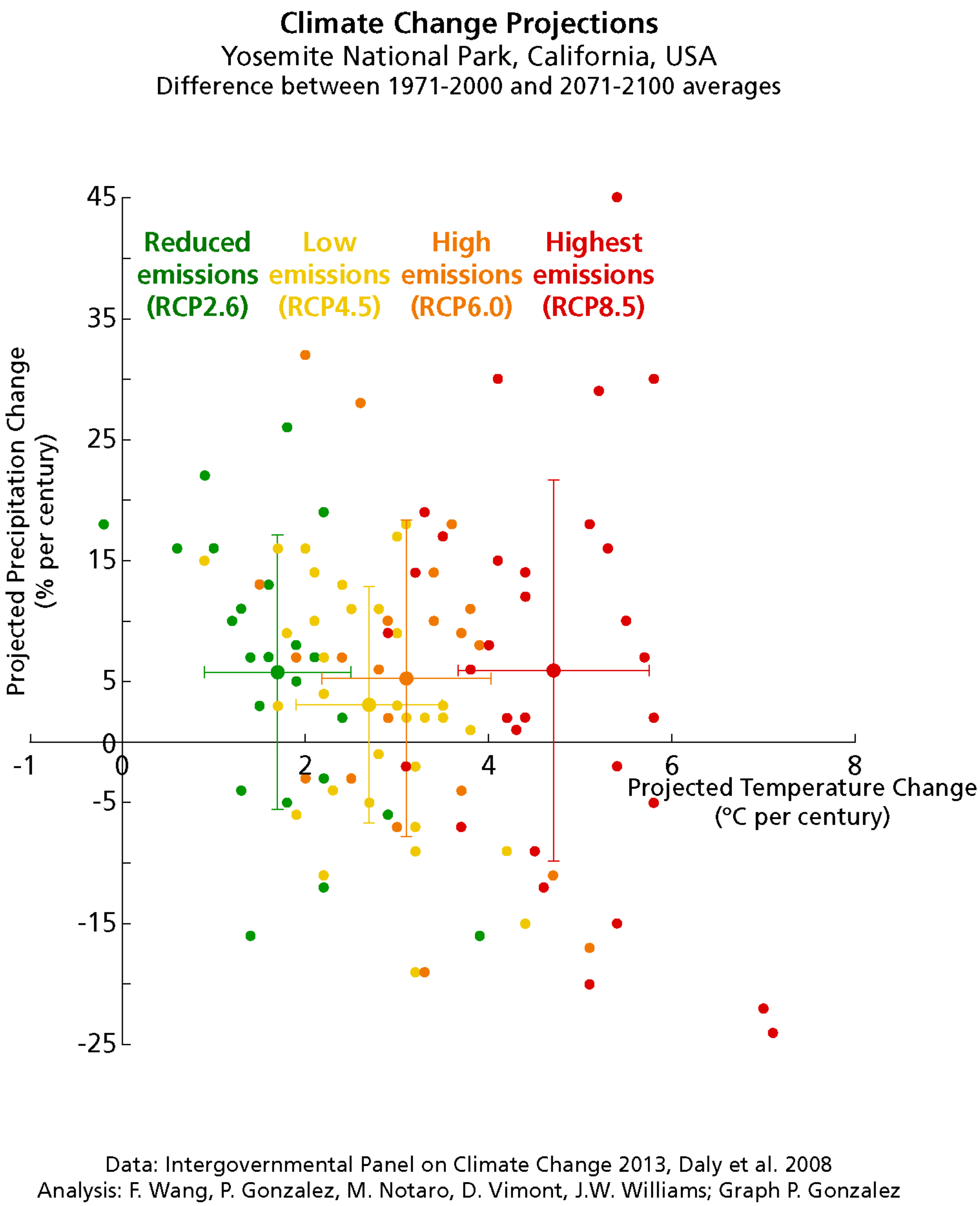

Projections of future climate for the area within park boundaries, relative to 1971-2000 average values. Each small dot is the output of a single GCM. The large color dots are the average values for the four IPCC emissions scenarios. The lines are the standard deviations of each emissions scenario average.

Figure 6.

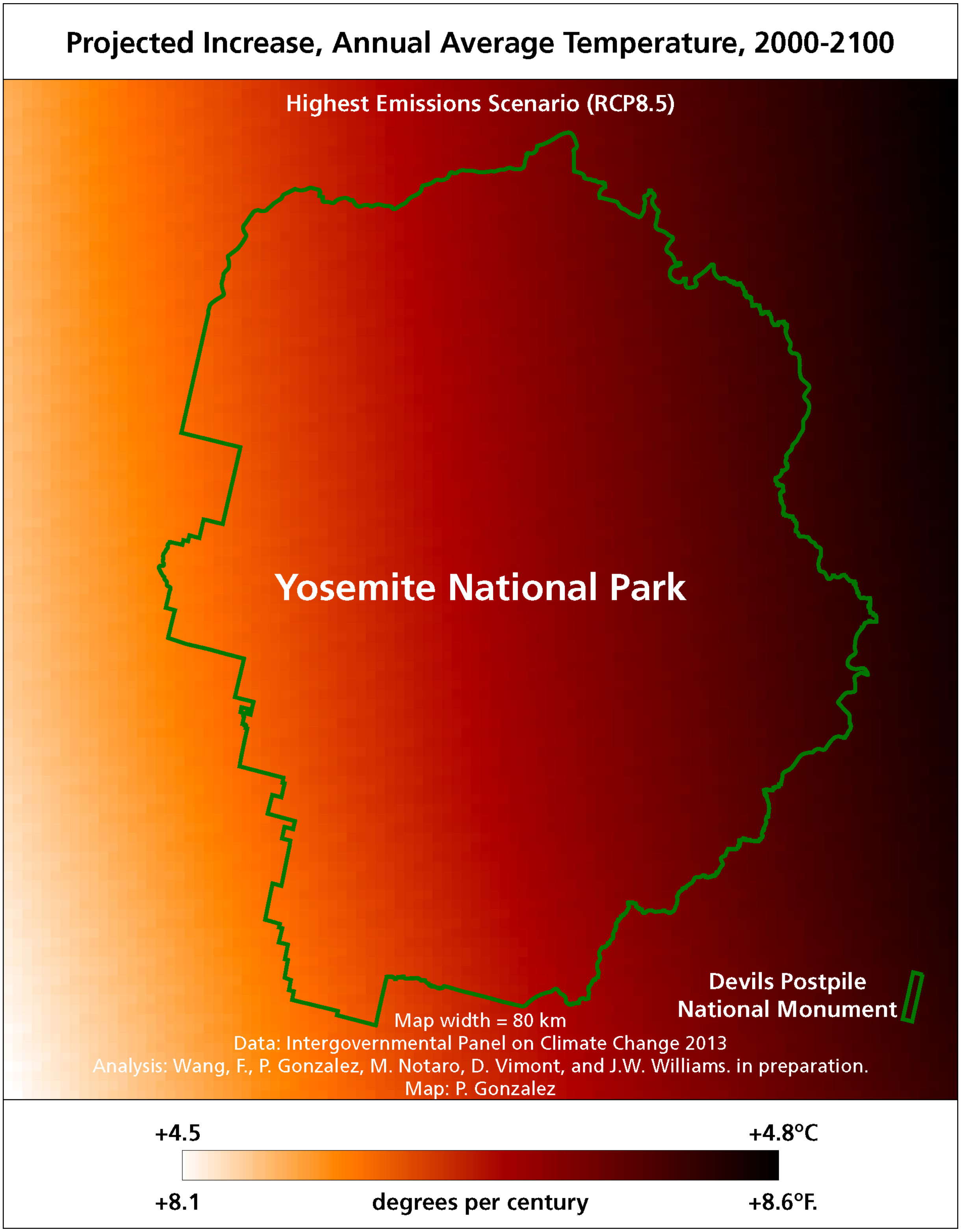

Minimum 4.5°C, Maximum 4.8°C per century

Figure 7.

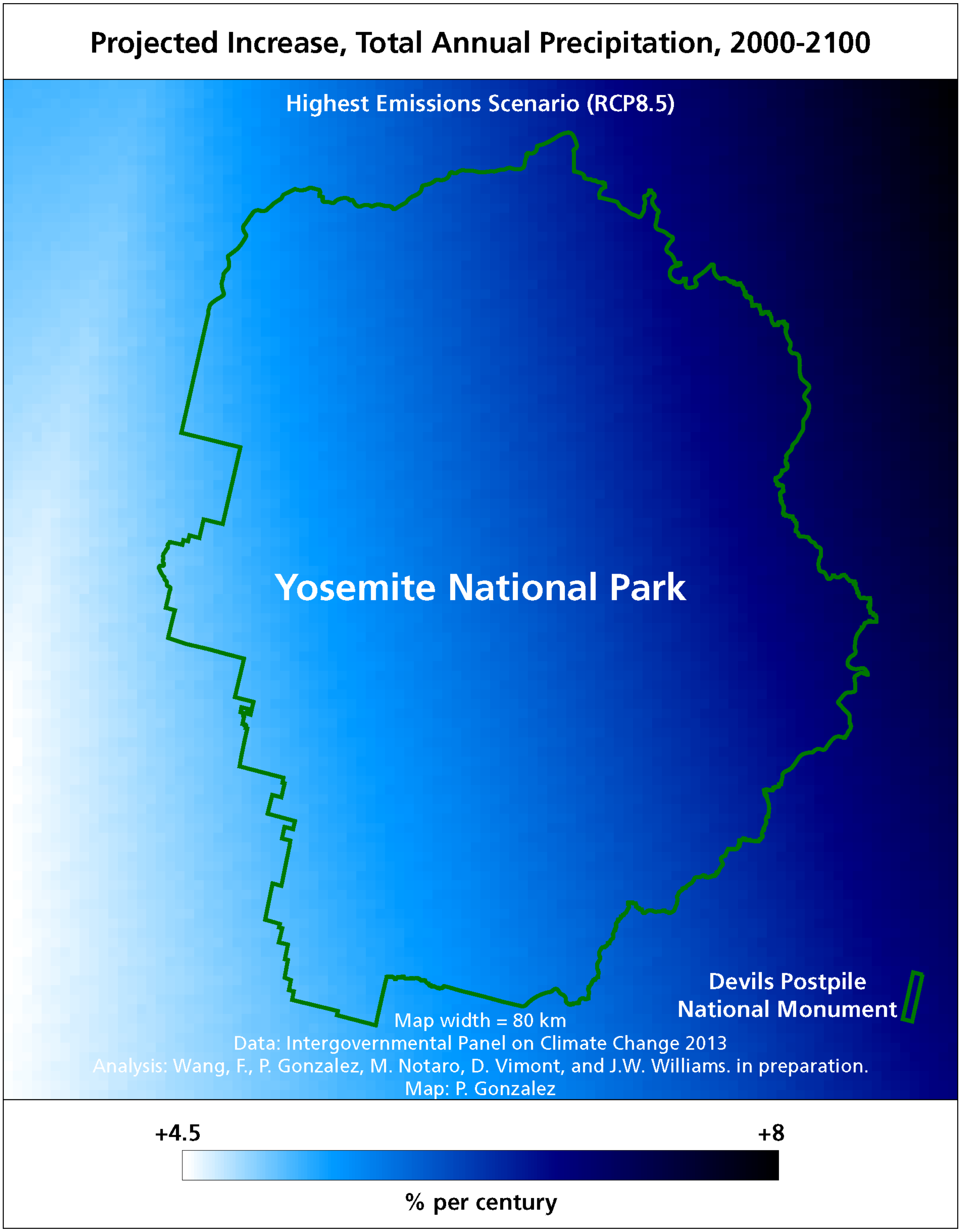

Minimum 4.5%, Maximum 8% per century

Figure 8.

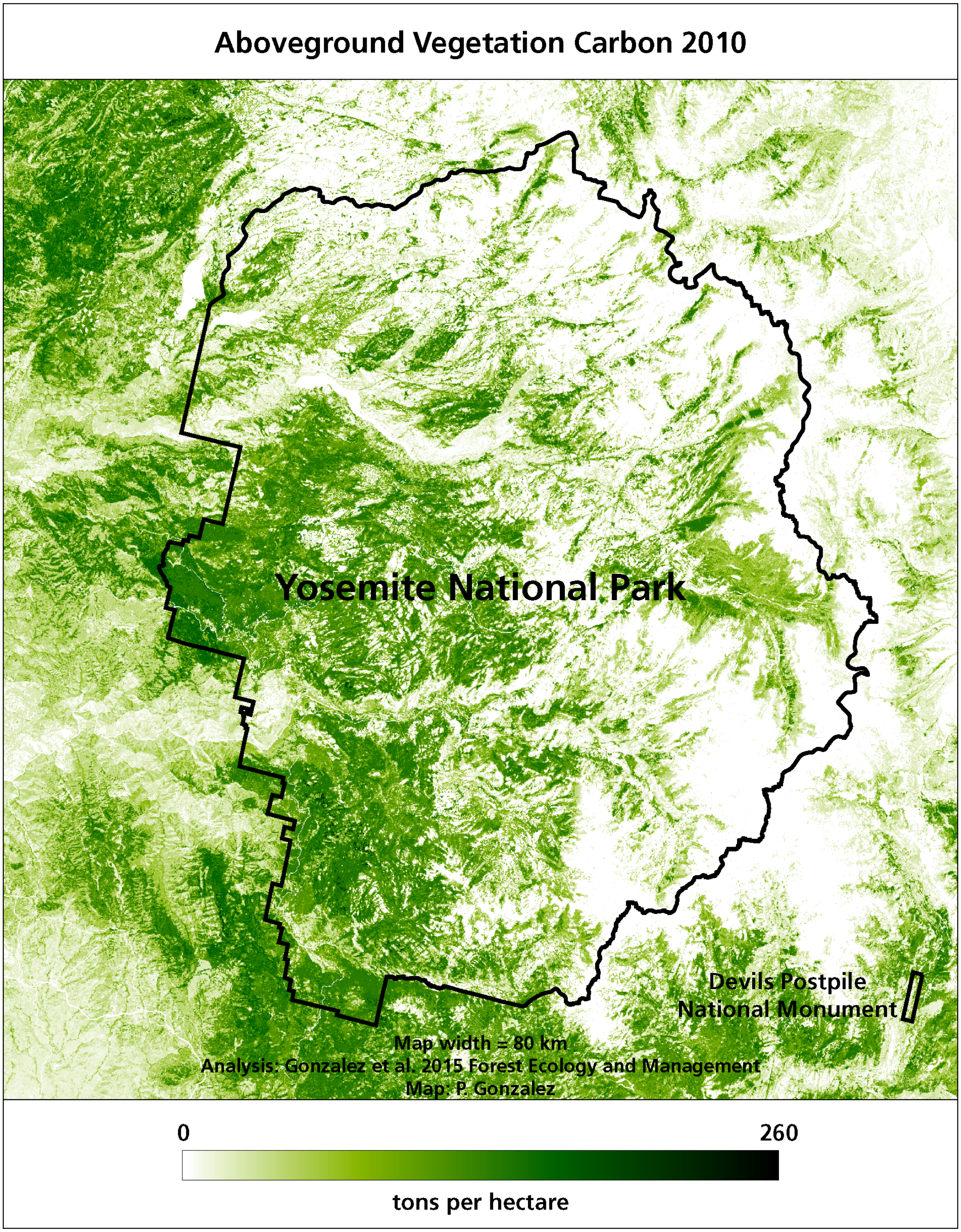

Minimum 0, Maximum 260 tons per hectare

Figure 9.

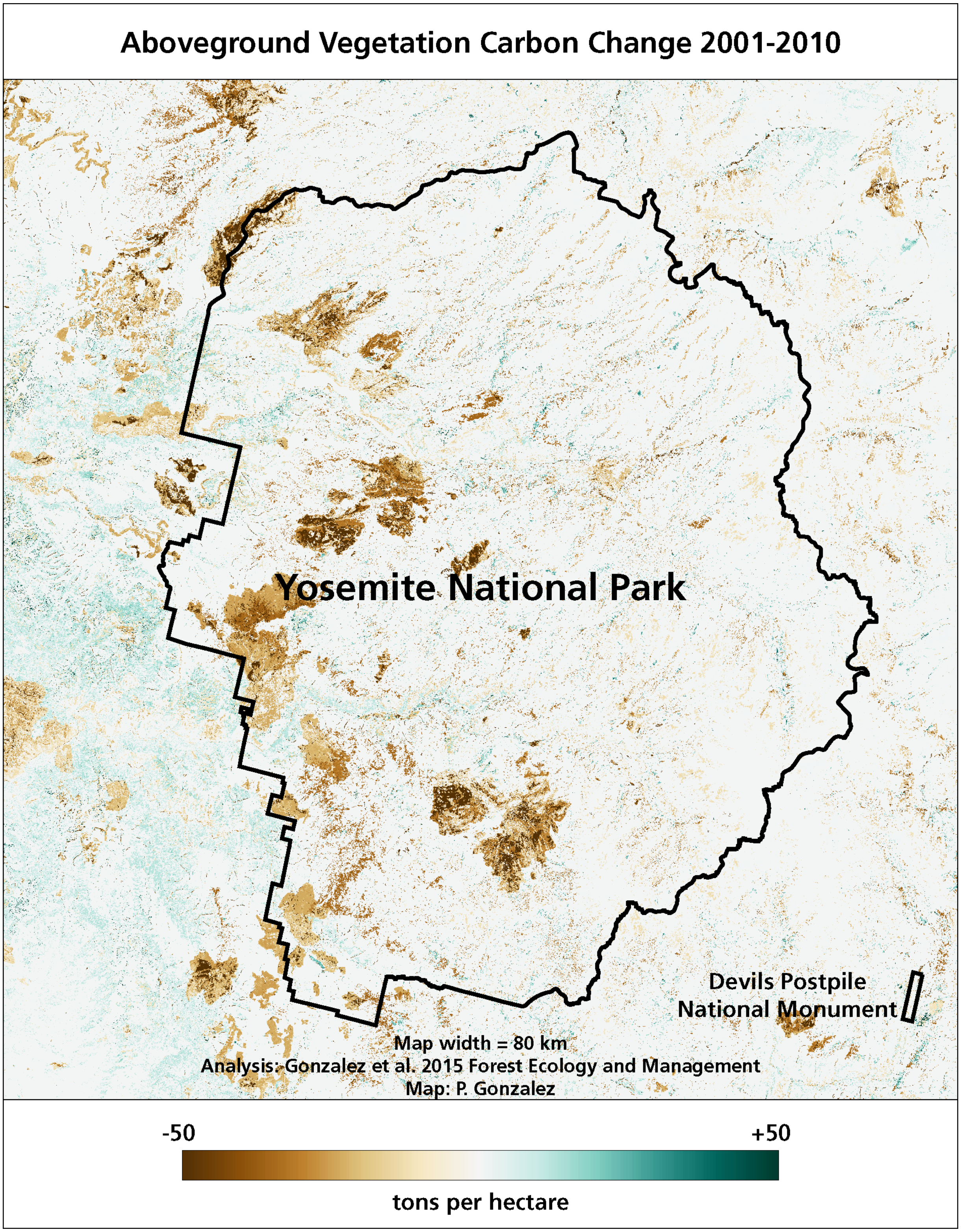

Minimum -260, Maximum +140 tons per hectare

Table 1. **Historical average temperatures** and temperature trends of the area within the boundaries of Yosemite National Park. SD = standard deviation, SE = standard error, sig. = statistical significance, * $P \leq 0.05$, ** $P \leq 0.01$, *** $P \leq 0.001$.

	1971-2000		1895-2010			1950-2010		
	mean	SD	trend	SE	sig.	trend	SE	sig.
	ºC		ºC century^{-1}			ºC century^{-1}		
Annual	5.5	0.6	0.6	0.2	*	1.9	0.7	**
December-February	-1	1.3	0.7	0.4		1.5	0.8	
March-May	3	1.4	0.6	0.3		2.8	0.9	**
June-August	13.2	0.9	0.5	0.3		2.4	1	*
September-November	6.8	1.3	0.6	0.3		0.9	0.9	
January	-1.1	1.6	1.2	0.5	*	3.7	1.1	**
February	-1.1	1.7	0.8	0.5		1.1	1	
March	0.3	1.9	0.8	0.6		4.6	1.3	***
April	2.5	2.1	-0.1	0.5		1.1	1.4	
May	6.2	2	1	0.5	*	2.7	1.1	*
June	10.9	1.5	0.5	0.5		2.5	1.4	
July	14.5	1.2	0.5	0.4		2.4	1.3	
August	14.3	1.2	0.5	0.3		2.4	0.9	**
September	11.5	1.6	1.1	0.5	*	1.7	1.2	
October	6.9	1.8	0.8	0.4		0.2	1.2	
November	1.9	2	-0.2	0.5		0.8	1.3	
December	-0.7	2	0.2	0.6		-0.3	1.7	

Table 2. **Historical average precipitation** totals and precipitation trends of the area within the boundaries of Yosemite National Park. No trends were statistically significant.
SD = standard deviation, SE = standard error.

	1971-2000		1895-2010		1950-2010	
	mean	SD	trend	SE	trend	SE
	mm y^{-1}		% $century^{-1}$		% $century^{-1}$	
Annual	1192	417	-1	9	5	28
December-February	632	326	2	13	8	34
March-May	310	172	-14	13	9	32
June-August	36	19	9	19	-56	43
September-November	225	133	10	20	-12	54
January	245	189	-16	23	8	60
February	191	139	-4	19	59	49
March	180	133	-28	21	13	45
April	76	54	9	18	-32	41
May	53	41	-8	22	67	56
June	18	14	-10	28	-36	69
July	11	14	41	28	-76	61
August	7	9	13	34	-73	93
September	23	26	-27	35	-74	98
October	68	54	7	27	111	71
November	134	103	17	25	-62	72
December	186	147	28	22	-20	60

Table 3. **Projected temperature increases** (°C), 2000 to 2050, for the area within Yosemite N.P. boundaries, from the average of all available general circulation model projections used for IPCC (2013). RCP = representative concentration pathway, SD = standard deviation.

	Emissions Scenarios							
	Reductions RCP2.6		Low RCP4.5		High RCP6.0		Highest RCP8.5	
	mean	SD	mean	SD	mean	SD	mean	SD
Annual	1.7	0.6	2	0.5	1.9	0.5	2.6	0.6
December-February	1.5	0.6	1.8	0.5	1.6	0.5	2.3	0.7
March-May	1.5	0.6	1.7	0.9	1.6	0.6	2.1	0.9
June-August	1.8	0.8	2.2	0.9	2.1	0.7	3	0.9
September-November	1.7	0.6	2.4	1.3	2	0.6	3.1	1.5
January	1.6	0.7	1.9	0.6	1.7	0.6	2.3	0.7
February	1.6	0.7	1.7	0.7	1.6	0.7	2	0.7
March	1.5	0.6	1.7	0.7	1.5	0.7	2	0.8
April	1.4	0.7	1.6	1	1.7	0.6	2.1	1
May	1.7	0.6	1.9	1.2	1.8	0.6	2.4	1.1
June	1.7	0.9	2	1.4	1.9	0.8	2.7	1.4
July	1.8	1	2.2	1.1	2.1	0.8	2.9	1.1
August	2	0.8	2.5	0.7	2.3	0.6	3.3	0.7
September	1.9	0.8	2.6	1.2	2.3	0.7	3.4	1.2
October	1.7	0.7	2.3	1.5	2	0.6	3.2	1.6
November	1.5	0.7	2.2	1.6	1.8	0.7	2.8	1.8
December	1.4	0.5	1.9	1	1.6	0.5	2.5	1.1

Table 4. **Projected temperature increases** (°C), 2000 to 2100, for the area within Yosemite N.P. boundaries, from the average of all available general circulation model projections used for IPCC (2013). RCP = representative concentration pathway, SD = standard deviation.

	Emissions Scenarios							
	Reductions RCP2.6		Low RCP4.5		High RCP6.0		Highest RCP8.5	
	mean	SD	mean	SD	mean	SD	mean	SD
Annual	1.7	0.8	2.7	0.8	3.1	0.9	4.7	1
December-February	1.7	0.7	2.4	0.7	2.8	0.8	4.1	1
March-May	1.6	0.8	2.2	1	2.8	0.9	4	1.1
June-August	1.7	1.1	3	1.1	3.5	1.1	5.3	1.2
September-November	1.8	0.9	3.2	1.6	3.4	1	5.5	1.9
January	1.8	0.8	2.4	0.8	2.8	0.8	4.1	1
February	1.6	0.8	2.3	0.8	2.8	0.8	3.9	1
March	1.6	0.9	2.1	0.9	2.6	0.9	3.8	1.1
April	1.5	0.8	2.1	1	2.6	0.8	3.8	1.1
May	1.6	0.8	2.5	1.2	3	1.1	4.4	1.5
June	1.7	1.2	2.7	1.6	3.3	1.4	5	1.6
July	1.7	1.2	2.9	1.4	3.5	1.3	5.2	1.4
August	1.8	1	3.2	1	3.7	1	5.7	1
September	2	1	3.4	1.4	3.8	1.1	5.9	1.6
October	1.8	1	3.2	1.7	3.4	1.1	5.6	2
November	1.6	0.8	2.8	1.8	3.1	1.1	4.9	2.1
December	1.6	0.6	2.5	1.2	2.7	0.9	4.2	1.5

Table 5. **Projected precipitation changes** (%), 2000 to 2050, for the area within Yosemite N.P. boundaries, from the average of all available general circulation model projections used for IPCC (2013). RCP = representative concentration pathway, SD = standard deviation.

	Emissions Scenarios							
	Reductions RCP2.6		Low RCP4.5		High RCP6.0		Highest RCP8.5	
	mean	SD	mean	SD	mean	SD	mean	SD
Annual	6	10	2	9	3	11	4	12
December-February	8	15	6	15	8	18	10	17
March-May	4	12	-1	13	0	14	0	16
June-August	16	32	16	29	5	24	12	35
September-November	1	14	-5	21	-2	17	-8	17
January	13	22	9	19	9	21	16	23
February	7	24	5	19	9	31	10	26
March	8	16	2	16	4	17	7	23
April	2	20	-1	20	-5	15	-2	22
May	-5	23	-10	27	-3	27	-11	29
June	1	29	-5	33	-3	29	-6	44
July	27	49	30	55	16	44	19	49
August	42	79	48	70	16	62	42	68
September	13	26	15	39	11	34	2	33
October	10	34	-1	28	6	34	-1	37
November	-4	16	-11	31	-7	20	-12	23
December	8	22	5	22	9	24	7	23

Table 6. **Projected precipitation changes** (%), 2000 to 2100, for the area within Yosemite N.P. boundaries, from the average of all available general circulation model projections used for IPCC (2013). RCP = representative concentration pathway, SD = standard deviation.

	Emissions Scenarios							
	Reductions RCP2.6		Low RCP4.5		High RCP6.0		Highest RCP8.5	
	mean	SD	mean	SD	mean	SD	mean	SD
Annual	6	11	3	10	5	13	6	16
December-February	6	15	9	16	11	20	17	24
March-May	8	13	-2	13	2	13	-6	15
June-August	15	32	19	38	9	32	22	54
September-November	1	15	-6	20	-5	18	-9	19
January	8	20	15	23	12	25	24	31
February	8	25	13	24	16	34	23	37
March	7	19	2	15	10	21	5	20
April	11	22	-2	20	-5	18	-13	20
May	7	25	-10	26	-10	23	-24	27
June	6	38	-2	41	-10	29	-17	34
July	18	37	34	60	25	55	44	92
August	32	57	50	74	36	66	86	125
September	12	40	17	50	9	31	24	52
October	14	36	-8	26	4	36	-7	31
November	-7	16	-9	25	-11	19	-16	26
December	5	22	-1	23	9	24	6	23

Table 7. **Ecosystem Carbon**. Aboveground carbon (mean ± 95% confidence interval) and surface area of changes in Yosemite National Park (Gonzalez et al. 2015).

Carbon stock 2010	14.8 ± 7.9	million tons
Carbon density 2010	50 ± 27	tons ha^{-1}
Change 2001-2010	-1.3 ± 0.6	million tons
Change 2001-2010	-8 ± 4	% of amount
Carbon increase	8	% of area
Carbon decrease	15	% of area

References

Arnold, C., T.A. Ghezzehei, and A.A. Berhe. 2014. Early Spring, severe frost events, and drought induce rapid carbon loss in high elevation meadows. PLoS ONE 9: e106058. doi:10.1371/journal.pone.0106058.

Ault, T.R., A.K. Macalady, G.T. Pederson, J.L. Betancourt, and M.D. Schwartz. 2011. Northern Hemisphere modes of variability and the timing of spring in western North America. Journal of Climate 24: 4003-4014.

Barnett, T.P., D.W. Pierce, H.G. Hidalgo, C. Bonfils, B.D. Santer, T. Das, G. Bala, A.W. Wood, T. Nozawa, A.A. Mirin, D.R. Cayan, and M.D. Dettinger. 2008. Human-induced changes in the hydrology of the western United States. Science 319: 1080-1083.

Blackard, J.A., M.V. Finco, E.H. Helmer, G.R. Holden, M.L. Hoppus, D.M. Jacobs, A.J. Lister, G.G. Moisen, M.D. Nelson, R. Riemann, B. Ruefenacht, D. Salajanu, D.L Weyermann, K.C. Winterberger, T.J. Brandeis, R.L. Czaplewski, R.E. McRoberts, P.L. Patterson, and R.P. Tymcio. 2008. Mapping U.S. forest biomass using nationwide forest inventory data and moderate resolution information. Remote Sensing of Environment 112: 1658-1677.

Bonfils, C., B.D. Santer, D.W. Pierce, H.G. Hidalgo, G. Bala, T. Das, T.P. Barnett, D.R. Cayan, C. Doutriaux, A.W. Wood, A. Mirin, and T. Nozawa. 2008. Detection and attribution of temperature changes in the mountainous western United States. Journal of Climate 21: 6404-6424.

Bradley, B.A., M. Oppenheimer, and D.S. Wilcove. 2009. Climate change and plant invasions: Restoration opportunities ahead? Global Change Biology 15: 1511-1521.

Bunn, A.G., L.J. Graumlich, and D.L. Urban. 2005. Trends in twentieth-century tree growth at high elevations in the Sierra Nevada and White Mountains, USA. Holocene 15: 481-488.

Burns, C.E., K.M. Johnston, and O.J. Schmitz. 2003. Global climate change and mammalian species diversity in US national parks. Proceedings of the National Academy of Sciences of the USA 100: 11 474-11 477.

Cristea, N.C., J.D. Lundquist, S.P. Loheide, C.S. Lowry, and C.E. Moore. 2014. Modelling how vegetation cover affects climate change impacts on streamflow timing and magnitude in the snowmelt-dominated upper Tuolumne Basin, Sierra Nevada. Hydrological Processes 28: 3896-3918.

Daly, C., M. Halbleib, J.I. Smith, W.P. Gibson, M.K. Doggett, G.H. Taylor, J. Curtis, and P.P. Pasteris. 2008. Physiographically sensitive mapping of climatological temperature and precipitation across the conterminous United States. International Journal of Climatology

28: 2031-2064.

Davey, C.A., K.T. Redmond, and D.B. Simeral. 2007. Weather and Climate Inventory, National Park Service, Sierra Nevada Network. National Park Service report NPS/SIEN/NRTR—2007/042. National Park Service, Fort Collins, Colorado.

Dolanc, C.R., J.H. Thorne, and H.D. Safford. 2013. Widespread shifts in the demographic structure of subalpine forests in the Sierra Nevada, California, 1934 to 2007. Global Ecology and Biogeography 22: 264-276.

Drexler, J.Z., D. Knifong, J. Tuil, L.E. Flint, and A.L. Flint. 2013. Fens as whole-ecosystem gauges of groundwater recharge under climate change. Journal of Hydrology 481: 22-34.

Drexler, J.Z., C.C. Fuller, J. Orlando, and P.E. Moore. 2015. Recent rates of carbon accumulation in montane fens of Yosemite National Park, California, U.S.A. Arctic, Antarctic, and Alpine Research 47: 657-669.

Earles, J.M., M.P. North, and M.D. Hurteau. 2014. Wildfire and drought dynamics destabilize carbon stores of fire-suppressed forests. Ecological Applications, 24: 732-740.

Eastman, L.M., T.L. Morelli, K.C. Rowe, C.J. Conroy, and C. Moritz. 2012. Size increase in high elevation ground squirrels over the last century. Global Change Biology 18: 1499-1508.

Edwards, L. M., and K. T. Redmond. 2011. Climate assessment for the Sierra Nevada Network Parks. National Park Service report NPS/2011/NRR—2011/482. National Park Service, Fort Collins, Colorado.

Eigenbrod, F., P. Gonzalez, J. Dash, and I. Steyl. 2015. Vulnerability of ecosystems to climate change moderated by habitat intactness. Global Change Biology 21: 275-286.

Godsey, S.E., J.W. Kirchner, and C.L. Tague. 2014. Effects of changes in winter snowpacks on summer low flows: Case studies in the Sierra Nevada, California, USA. Hydrological Processes 28: 5048-5064.

Gonzalez, P., J.J. Battles, B.M. Collins, T. Robards, and D.S. Saah. 2015. Aboveground live carbon stock changes of California wildland ecosystems, 2001-2010. Forest Ecology and Management 348: 68-77.

Gonzalez, P., G.P. Asner, J.J. Battles, M.A. Lefsky, K.M. Waring, and M. Palace. 2010a. Forest carbon densities and uncertainties from Lidar, QuickBird, and field measurements in California. Remote Sensing of Environment 114: 1561-1575.

Gonzalez, P., R.P. Neilson, J.M. Lenihan, and R.J. Drapek. 2010b. Global patterns in the vulnerability of ecosystems to vegetation shifts due to climate change. Global Ecology and Biogeography 19: 755-768.

Hurteau, M.D., J.B. Bradford, P.Z. Fulé, A.H. Taylor, and K.L. Martin. 2014. Climate change, fire management, and ecological services in the southwestern US. Forest Ecology and Management 327: 280-289.

Hurteau, M.D. and M.L. Brooks. 2011. Short- and long-term effects of fire on carbon in US dry temperate forest systems. BioScience 61: 139-146.

Hurteau, M. and M. North. 2009a. Response of *Arnica dealbata* to climate change, nitrogen deposition, and fire. Plant Ecology 202: 191-194.

Hurteau, M. and M. North. 2009b. Fuel treatment effects on tree-based forest carbon storage and emissions under modeled wildfire scenarios. Frontiers in Ecology and the Environment 7: 409-414.

Intergovernmental Panel on Climate Change (IPCC). 2000. Emissions Scenarios. Cambridge University Press, Cambridge, UK.

Intergovernmental Panel on Climate Change (IPCC). 2013. Climate Change 2013: The Physical Science Basis. Cambridge University Press, Cambridge, UK.

Intergovernmental Panel on Climate Change (IPCC). 2014. Climate Change 2014: Impacts, Adaptation, and Vulnerability. Cambridge University Press, Cambridge, UK.

La Sorte, F.A. and F.R. Thompson. 2007. Poleward shifts in winter ranges of North American birds. Ecology 88: 1803-1812.

Lawrimore, J.H., M.J. Menne, B.E. Gleason, C.N. Williams, D.B. Wuertz, R.S. Vose, and J. Rennie. 2011. An overview of the Global Historical Climatology Network monthly mean temperature data set, version 3. Journal of Geophysical Resesearch: Atmospheres 116: D19121. doi:10.1029/2011JD016187.

Littell, J.S., D. McKenzie, D.L. Peterson, and A.L. Westerling. 2009. Climate and wildfire area burned in western U.S. ecoprovinces, 1916–2003. Ecological Applications 19: 1003-1021.

Lutz, J.A., J.W. van Wagtendonk, J.F. Franklin. 2009a. Twentieth-century decline of large-diameter trees in Yosemite National Park, California, USA. Forest Ecology and Management 257: 2296-2307.

Lutz, J.A., J.W. van Wagtendonk, A.E. Thode, J.D. Miller, and J.F. Franklin. 2009b. Climate, lightning ignitions, and fire severity in Yosemite National Park, California, USA. International Journal of Wildland Fire 18: 765-774.

Lutz, J.A., J.W. van Wagtendonk, J.F. Franklin. 2010. Climatic water deficit, tree species ranges, and climate change in Yosemite National Park. Journal of Biogeography 37: 936-950.

Marlon, J.R., P.J. Bartlein, D.G. Gavin, C.J. Long, R.S. Anderson, C.E. Briles, K.J. Brown, D.

Colombaroli, D.J. Hallett, M.J. Power, E.A. Scharf, and M.K. Walsh. 2012. Long-term perspective on wildfires in the western USA. Proceedings of the National Academy of Sciences of the USA 109: E535-E543.

Matchett, J.R., J.A. Lutz, L.W. Tarnay, D.G. Smith, K.M.L. Becker, and M.L. Brooks. 2015. Impacts of fire management on aboveground tree carbon stocks in Yosemite and Sequoia & Kings Canyon National Parks. National Park Service report NPS/SIEN/NRR—2015/910. National Park Service, Fort Collins, Colorado.

McIntyre, P.J., J.H. Thorne, C.R. Dolanc, A.L. Flint, L.E. Flint, M. Kelly, and D.D. Ackerly. 2015. Twentieth-century shifts in forest structure in California: Denser forests, smaller trees, and increased dominance of oaks. Proceedings of the National Academy of Sciences of the USA 112: 1458-1463.

Millar, C.I., R.D. Westfall, D.L. Delany, J.C. King, and L.J. Graumlich. 2004. Response of subalpine conifers in the Sierra Nevada, California, U.S.A., to 20th-Century warming and decadal climate variability. Arctic, Antarctic, and Alpine Research 36: 181-200.

Morelli, T.L., A.B. Smith, C.R. Kastely, I. Mastroserio, C. Moritz, and S.R. Beissinger. 2012. Anthropogenic refugia ameliorate the severe climate-related decline of a montane mammal along its trailing edge. Proceedings of the Royal Society of London B 279: 4279-4286.

Moritz, C., J.L. Patton, C.J. Conroy, J.L. Parra, G.C. White, and S.R. Beissinger. 2008. Impact of a century of climate change on small-mammal communities in Yosemite National Park, USA. Science 322: 261-264.

Moritz, M.A., M.A. Parisien, E. Batllori, M.A. Krawchuk, J. Van Dorn, D.J. Ganz, and K. Hayhoe. 2012. Climate change and disruptions to global fire activity. Ecosphere 3: art49. doi:10.1890/ES11-00345.1.

Moss, R.H., J.A. Edmonds, K.A. Hibbard, M.R. Manning, S.K. Rose, D.P. van Vuuren, T.R. Carter, S. Emori, M. Kainuma, T. Kram, G.A. Meehl, J.F.B. Mitchell, N. Nakicenovic, K. Riahi, S.J. Smith, R.J. Stouffer, A.M. Thomson, J.P. Weyant, and T.J. Wilbanks. 2010. The next generation of scenarios for climate change research and assessment. Nature 463: 747-756.

Null, S.E., J.H. Viers, M.L. Deas, S.K. Tanaka, and J.F. Mount. 2013. Stream temperature sensitivity to climate warming in California's Sierra Nevada: impacts to coldwater habitat. Climatic Change 116: 149-170.

Pierce, D.W., T.P., Barnett, H.G. Hidalgo. T. Das, C. Bonfils, B.D. Santer, G. Bala, M.D.

Dettinger, D.R. Cayan, A. Mirin, A.W. Wood, and T. Nozawa. 2008. Attribution of declining western U.S. snowpack to human effects. Journal of Climate 21: 6425-6444.

Rowe, C.M. and L.E. Derry. 2012. Trends in record-breaking temperatures for the conterminous United States. Geophysical Research Letters 39: L16703. doi:10.1029/2012GL052775.

Rubidge, E.M., W.B. Monahan, J.L. Parra, S.E. Cameron, and J.S. Brashares. 2011. The role of climate, habitat, and species co-occurrence as drivers of change in small mammal distributions over the past century. Global Change Biology 17: 696–708.

Rubidge, E.M., J.L. Patton, M. Lim, A.C. Burton, J.S. Brashares, and C. Moritz. 2012. Climate-induced range contraction drives genetic erosion in an alpine mammal. Nature Climate Change 2: 285-288.

Santos, M.J., J.H. Thorne, and C. Moritz. 2015. Synchronicity in elevation range shifts among small mammals and vegetation over the last century is stronger for omnivores. Ecography 38: 556-568.

Schwartz, M.W., N. Butt, C.R. Dolanc, A. Holguin, M.A. Moritz, M.P. North, H.D. Safford, N.L. Stephenson, J.H. Thorne, and P.J. van Mantgem. 2015. Increasing elevation of fire in the Sierra Nevada and implications for forest change. Ecosphere 6(7):121. doi:10.1890/ES15-00003.1.

Siegel, R.B., P. Pyle, J.H. Thorne, A.J. Holguin, C.A. Howell, S. Stock, and M.W. Tingley. 2014. Vulnerability of birds to climate change in California's Sierra Nevada. Avian Conservation and Ecology 9: 7. doi:10.5751/ACE-00658-090107.

Stephens, S.L., J.K. Agee, P.Z. Fulé, M.P. North, W.H. Romme, T.W. Swetnam, and M.G. Turner. 2013. Managing forests and fire in changing climates. Science 342: 41-42.

Stephens, S.L., R.E. Martin, and N.E. Clinton. 2007. Prehistoric fire area and emissions from California's forests, woodlands, shrublands, and grasslands. Forest Ecology and Management 251: 205-216.

Stewart, J.A.E., J.D. Perrine, L.B. Nichols, J.H. Thorne, C.I. Millar, K.E. Goehring, C.P. Massing, and D.H. Wright. 2015. Revisiting the past to foretell the future: Summer temperature and habitat area predict pika extirpations in California. Journal of Biogeography 42: 880-890.

Swetnam, T.W. 1993. Fire history and climate change in giant sequoia groves. Science 262: 885-889.

Swetnam, T.W., C.H. Baisan, A.C. Caprio, P.M. Brown, R. Touchan, R.S. Anderson, and D.J. Hallett. 2009. Multi-millennial fire history of the Giant Forest, Sequoia National Park, California, USA. Fire Ecology 5: 120-150.

Taylor, A.H. and A.E. Scholl. 2012. Climatic and human influences on fire regimes in mixed conifer forests in Yosemite National Park, USA. Forest Ecology and Management 267: 144-156.

Tingley, M.W., M.S. Koo, C. Moritz, A.C. Rush, and S.R. Beissinger. 2012. The push and pull of climate change causes heterogeneous shifts in avian elevational ranges. Global Change Biology 18: 3279-3290.

Tingley, M.W., W.B. Monahan, S.R. Beissinger, and C. Moritz. 2009. Birds track their Grinnellian niche through a century of climate change. Proceedings of the National Academy of Sciences of the United States of America 106: 19 637-19 643.

Trouet, V., A.H. Taylor, E.R. Wahl, C.N. Skinner, and S.L. Stephens. 2010. Fire-climate interactions in the American West since 1400 CE. Geophysical Research Letters 37: L04702. doi:10.1029/2009GL041695.

van Mantgem, P.J., N.L. Stephenson, J.C. Byrne, L.D. Daniels, J.F. Franklin, P.Z. Fule, M.E. Harmon, A.J. Larson, J.M. Smith, A.H. Taylor, and T.T. Veblen. 2009. Widespread increase of tree mortality rates in the western United States. Science 323: 521-524.

Villalba, G., L. Tarnay, E. Campbell, and X. Gabarrell. 2013. A life-cycle carbon footprint of Yosemite National Park. Energy Policy 62: 1336-1343.

Walsh, J., D. Wuebbles, K. Hayhoe, J. Kossin, K. Kunkel, G. Stephens, P. Thorne, R. Vose, M. Wehner, and J. Willis. 2014. Our changing climate. In Melillo, J.M., T.C. Richmond, and G. W. Yohe (Eds.) Climate Change Impacts in the United States: The Third National Climate Assessment. U.S. Global Change Research Program, Washington, DC.

Wang, F., P. Gonzalez, M. Notaro, D. Vimont, and J.W. Williams. in preparation. Significant historical and projected climate change in U.S. national parks.

Westerling, A.L., B.P. Bryant, H.K. Preisler, T.P. Holmes, H.G. Hidalgo, T. Das, and S.R. Shrestha. 2011. Climate change and growth scenarios for California wildfire. Climatic Change 109: S445-463.

Wood, A.W., L.R. Leung, V. Sridhar and D.P. Lettenmaier. 2004. Hydrologic implications of dynamical and statistical approaches to downscaling climate model outputs. Climatic Change 62: 189-216.

Yang, D.S., C.J. Conroy, and C. Moritz. 2011. Contrasting responses of Peromyscus mice of Yosemite National Park to recent climate change. Global Change Biology 17: 2559-2566.